Imaging small numbers of Ba atoms in solid xenon for barium tagging in nEXO

T. Walton,[1] C. Chambers,[1] A. Craycraft,[1] W. Fairbank Jr.,[1,*] J.B. Albert,[2] D.J. Auty,[3] P.S. Barbeau,[4] V. Basque,[5] D. Beck,[6] M. Breidenbach,[7] T. Brunner,[8,9] G.F. Cao,[10] B. Cleveland,[11,†] M. Coon,[6] T. Daniels,[7] S.J. Daugherty,[2] R. DeVoe,[8] T. Didberidze,[3] J. Dilling,[12] M.J. Dolinski,[13] M. Dunford,[5] L. Fabris,[14] J. Farine,[11] W. Feldmeier,[15] P. Fierlinger,[15] D. Fudenberg,[8] G. Giroux,[16,‡] R. Gornea,[5,16] K. Graham,[5] G. Gratta,[8] M. Heffner,[17] M. Hughes,[3] X.S. Jiang,[10] T.N. Johnson,[2] S. Johnston,[18] A. Karelin,[19] L.J. Kaufman,[2] R. Killick,[5] T. Koffas,[5] S. Kravitz,[8] R. Krücken,[12] A. Kuchenkov,[19] K.S. Kumar,[20] D.S. Leonard,[21] C. Licciardi,[5] Y.H. Lin,[13] J. Ling,[6] R. MacLellan,[22] M.G. Marino,[15] B. Mong,[11] D. Moore,[8] A. Odian,[7] I. Ostrovskiy,[8] A. Piepke,[3] A. Pocar,[18] F. Retiere,[12] P.C. Rowson,[7] M.P. Rozo,[5] A. Schubert,[8] D. Sinclair,[12,5] E. Smith,[13] V. Stekhanov,[19] M. Tarka,[20] T. Tolba,[16] K. Twelker,[8,§] J.-L. Vuilleumier,[16] J. Walton,[6] M. Weber,[8] L.J. Wen,[10] U. Wichoski,[11] L. Yang,[6] Y.-R. Yen,[13] and Y.B. Zhao[10]

(nEXO Collaboration)

[1] *Physics Department, Colorado State University, Fort Collins CO, USA*
[2] *Physics Department and CEEM, Indiana University, Bloomington IN, USA*
[3] *Department of Physics and Astronomy, University of Alabama, Tuscaloosa AL, USA*
[4] *Department of Physics, Duke University, and Triangle Universities Nuclear Laboratory (TUNL), Durham North Carolina, USA*
[5] *Physics Department, Carleton University, Ottawa ON, Canada*
[6] *Physics Department, University of Illinois, Urbana-Champaign IL, USA*
[7] *SLAC National Accelerator Laboratory, Stanford CA, USA*
[8] *Physics Department, Stanford University, Stanford CA, USA*
[9] *Department of Physics, McGill University, Montreal QC, Canada*
[10] *Institute of High Energy Physics, Beijing, China*
[11] *Department of Physics, Laurentian University, Sudbury ON, Canada*
[12] *TRIUMF, Vancouver BC, Canada*
[13] *Department of Physics, Drexel University, Philadelphia PA, USA*
[14] *Oak Ridge National Laboratory, Oak Ridge TN, USA*
[15] *Technische Universitat Munchen, Physikdepartment and Excellence Cluster Universe, Garching, Germany*
[16] *LHEP, Albert Einstein Center, University of Bern, Bern, Switzerland*
[17] *Lawrence Livermore National Laboratory, Livermore CA, USA*
[18] *Amherst Center for Fundamental Interactions and Physics Department, University of Massachusetts, Amherst MA, USA*
[19] *Institute for Theoretical and Experimental Physics, Moscow, Russia*
[20] *Department of Physics and Astronomy, Stony Brook University, SUNY, Stony Brook NY,USA*
[21] *New place in S. Korea*
[22] *Department of Physics, University of South Dakota, Vermillion SD, USA*

(Dated: January 13, 2016)

Images of Ba atoms in solid Xe in a focused laser region, after deposition from vacuum onto a cold sapphire window, are obtained using a 619-nm fluorescence peak down to the single-atom level. This is an important step toward Ba tagging with a cryogenic probe from liquid Xe for the nEXO neutrinoless double beta decay experiment.

I. INTRODUCTION

The search for neutrinoless double beta decay ($0\nu\beta\beta$) is an important probe into the nature of neutrinos. Observation would require that neutrinos are Majorana particles, would demonstrate violation of lepton number conservation, and could help determine the absolute neutrino mass [1]. EXO-200 is searching for $0\nu\beta\beta$ in ^{136}Xe with around 170 kg of liquid Xe (lXe) enriched to 80.6% ^{136}Xe in a dual time projection chamber (TPC). Two-neutrino double beta decay ($2\nu\beta\beta$) of ^{136}Xe has been observed by EXO-200, and its half-life is measured at $T^{2\nu\beta\beta}_{1/2} = 2.165 \pm 0.016(\text{stat}) \pm 0.059(\text{sys}) \times 10^{21}$ yr [2].

* Corresponding author
† Also SNOLAB, Sudbury ON, Canada
‡ Now at Queen's University, Kingston ON, Canada
§ Now at WiTricity, Watertown, MA

The most recent EXO-200 $0\nu\beta\beta$ search sets a limit on the half-life at $T_{1/2}^{0\nu\beta\beta} < 1.1 \times 10^{25}$ yr (90% CL), which corresponds to an effective Majorana neutrino mass of $\langle m_{\nu_e} \rangle$ <190-450 meV, depending on nuclear matrix element calculations [3].

A lXe TPC provides a unique opportunity to tag the daughter at the site of a double beta decay event, called Ba tagging, which would improve $0\nu\beta\beta$ sensitivity by effectively eliminating all backgrounds [4]. Ba tagging is being investigated for possible incorporation in the next-generation ton-scale lXe experiment, nEXO. Initial results have been reported for research on methods of Ba tagging in lXe [5 and hot probe paper?] and also in a Xe gas TPC [6]. The method described here is for Ba tagging in the nEXO lXe TPC, in which a cryogenic probe would be moved to the position of the $0\nu\beta\beta$ candidate in order to freeze the daughter ion into a small amount of solid Xe (sXe) at the end of the probe. It would then be detected by its laser-induced fluorescence in the sXe.

The spectroscopy of Ba in sXe is described in the previous work [7]. An image of $\leq 10^4$ Ba atoms was obtained with the strong fluorescence peaks at 577 and 591 nm. However, bleaching of these fluorescence peaks with l exposure causes rapid reduction of the emissio these wavelengths at high laser intensity, e.g., using a focused beam. Thus obtaining large numbers of photons from single Ba atoms is difficult without a method to overcome bleaching, e.g., with repumping lasers. Imaging was not attempted in [7] with the peak at 619 nm, though this peak has weaker bleaching by many orders of magnitude. This peak is promising for imaging of smaller numbers of atoms because larger numbers of photons per atom may be obtained.

It is expected that a Ba^{++} ion will neutralize once to Ba^+ in lXe, as the lXe conduction band gap is slightly less than the ionization potential for Ba^+ [4]. Neutralization to Ba may also occur in the charge cloud following a $\beta\beta$ event. A new study of ^{214}Bi daughters of ^{214}Pb β-decay in EXO-200 has reported that 76(6)% of these daughters are ionized, with negligible subsequent neutralization after many minutes [8]. Thus, a high percentage of ^{136}Ba $0\nu\beta\beta$ daughters may be expected in the single ionized state in lXe. Whether or not the ^{136}Ba will remain ionized in sXe on a cold probe is not yet known. This work focuses on imaging single Ba atoms in sXe via the low-bleaching 619-nm fluorescence. Varying numbers of atoms are observed in a focused laser region down to the single atom level.

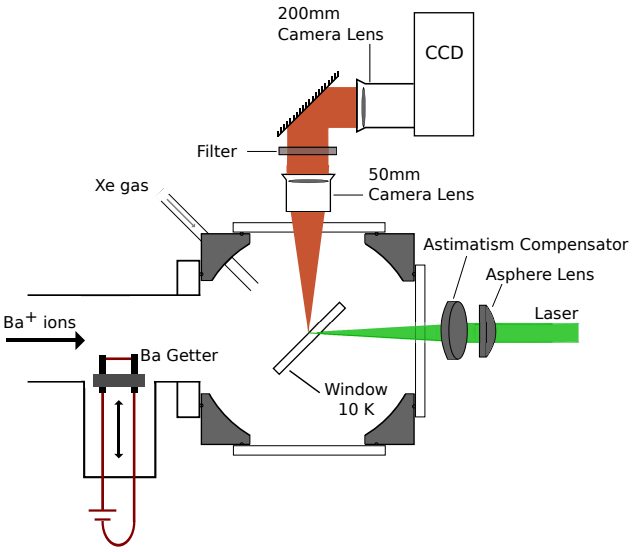

FIG. 1. Experimental setup for depositing Ba/Ba^+ in sXe matrices, and for excitation and observation.

II. APPARATUS AND METHOD

The apparatus for depositing and observing Ba/Ba^+ deposits in sXe is described in [7]. Important components are shown in Fig. 1. The source of Ba^+ is an ion beam at 2000 eV, filtered to select Ba^+ with an E×B velocity filter. A set of pulsing plates produces 1-μs pulses for depositing small numbers of ions. The spectra of Ba^+ ion deposits in the sXe matrix exhibit peaks known to be due to neutral Ba atoms [7]. Thus some percentage of the ions neutralize in the matrix, but the fraction has not yet been determined. An alternative source of neutral Ba is a $BaAl_4$ getter wire which can be inserted to emit Ba atoms toward the sample. However, it is challenging to achieve low Ba flux with this source and to calibrate it.

Deposits are made on a cold sapphire window tilted at 45°. To create a sample, Xe gas is directed toward the window using a leak valve. The Xe gas freezes on the window and forms a sXe matrix with a thickness of around half a micron. This is initiated a few seconds prior to the Ba deposit, continues during the Ba deposit, and is turned off a few seconds after the Ba deposit.

In this work, deposits are made with the sapphire window at around 50 K, partly to reduce hydrogen content in the matrix, as hydrogen condenses well below 50 K in vacuum [7]. The window is then cooled to 11 K for observation. Deposits made at 50 K result in higher 619-nm signal than those made

at 11 K. Xe deposition at around 30 nm/s also results in higher 619-nm signal, as compared to lower leak rates, while not being so high as to result in a frosty Xe matrix. An experiment cycle consists of a deposit at 50 K and a fluorescence observation at 11 K; then the deposit is evaporated by heating the window to 100 K. Many deposits are made in a day with varying numbers of ions deposited, as well as periodic Xe-only deposits to establish the background.

The excitation laser, a Coherent 599 cw dye laser with Rhodamine 6G dye pumped by the 514-nm line of a Lexel 3500 argon ion laser, enters from the back side of the window. Ba fluorescence light is collected and collimated by a 50 mm Nikon camera lens. A band-pass filter with FWHM of 20 nm passes just the 619-nm fluorescence peak. A 200 mm Nikon camera lens then focuses the image onto a liquid nitrogen cooled CCD, resulting in an image of 4× magnification. Each of the 20[illegible] μm [illegible]els of the CCD represents approximately [illegible]5 μm [illegible] the SXe sample.

For a given laser intensity, the smallest focus possible is desired for optimal signal-to-noise from single atoms. To achieve this, an aspherical lens of 7.9 cm focal length [9] is used to minimize spherical aberration, and a fused silica optical flat of 1 cm thickness is placed at 10° after the lens in order to compensate for astigmatism caused by the tilted sapphire window (see Fig. 1).

III. RESULTS

A typical image made with a focused laser beam at 570 nm is shown in Fig. 2. The laser's path through the sapphire window is seen as a weak vertical line. At both ends, some background emission from the surfaces is observed. At the front surface (at the top in the image), extra fluorescence is detected from a small number of Ba atoms within the focused laser.

The number of Ba^+ ions deposited within the 1/e radius of the laser beam gives a rough upper limit to the number of Ba atoms responsible for the observed signal. For typical ion pulses of 13 fC/pulse and focused laser $1/e^2$ radii of $w_{0x} = 2.06$ μm and $w_{0y} = 2.66$ μm, this results in about 0.035 Ba^+ ions/pulse in the 1/e intensity laser region. The signal in Fig. 2 corresponds to a deposit of about 10 Ba^+ ions into the laser region, and is therefore roughly due to ≤ 10 Ba atoms. Deposits of ≤ 39, ≤ 3, and ≤ 1 Ba atoms are shown in Fig. 3a,b,c, respectively, with Xe-only deposits made before and after each Ba^+ deposit. Background is determined by averaging the summed

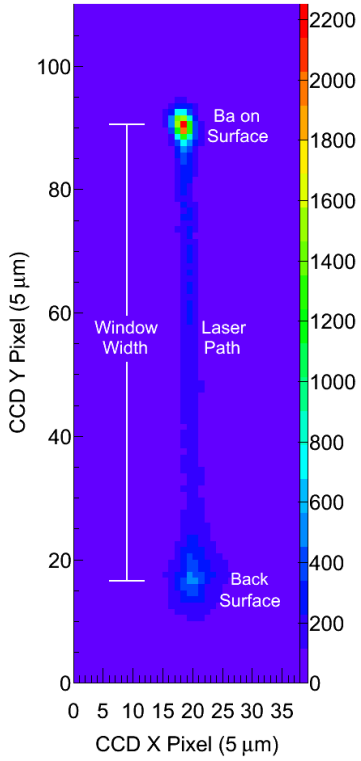

FIG. 2. Example image of a Ba^+ deposit in sXe on a tilted c-plane sapphire window of 0.5 mm thickness.

CCD counts in the focused laser region from the two surrounding Xe-only deposits for each Ba^+ deposit. The absence of Ba fluorescence in Xe-only deposits after evaporating the previous Ba deposit, shown for a large deposit of $\leq 6.1 \times 10^4$ Ba atoms in Fig. 4, is important for the implementation of this Ba tagging method in nEXO, i.e., false positives will not occur from p[illegible]ious B[illegible]gs.

The [illegible]unts v[illegible]ns deposited [illegible] plotted in Fig. 5. The summed CCD counts in the laser region in sXe of each image is linear with ions deposited, albeit with significant scatter due to ion beam instabilities in this run. The observed signal corresponds to 2200 ± 230 counts/mW per atom with around 0.24 mW of focused 570-nm laser excitation, and 60-s CCD exposures. Counts are scaled by laser power to account for small variations in laser power. Subtracted images of deposits near the linear trend line are shown in Fig. 6 corresponding to (a) ≤ 10 atoms, (a) ≤ 3 atoms, and (a) ≤ 1 atom. These represent the expected signal level, with a clear peak at the single-atom level.

A Gaussian fit to the images gives a $1/e^2$ radius of 12 μm, which is much larger than the average laser

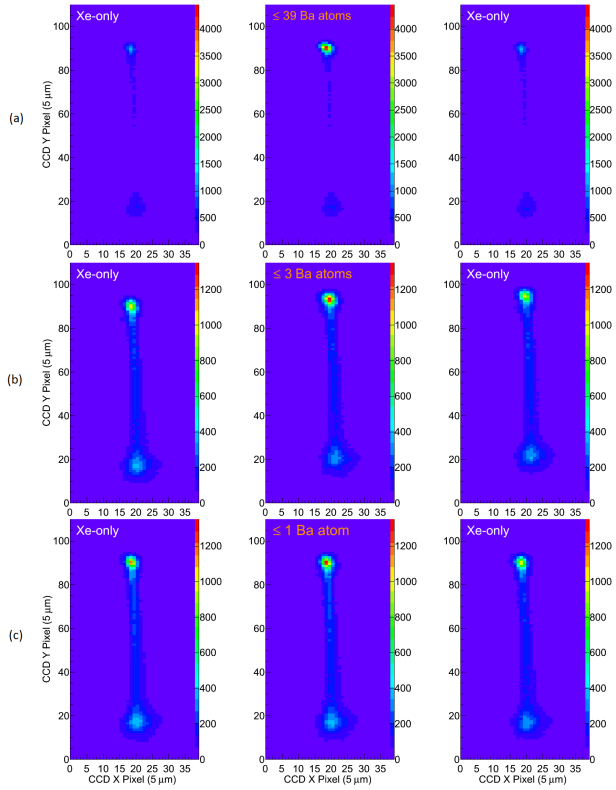

FIG. 3. Images of Ba^+ deposits yielding (a) ≤ 39, (b) ≤ 3, and (c) ≤ 1 Ba atoms in the focused laser region, with Xe-only deposits done before and after each respective Ba^+ deposit. Exposures are 60 s with around 0.24 mW of 570-nm laser excitation.

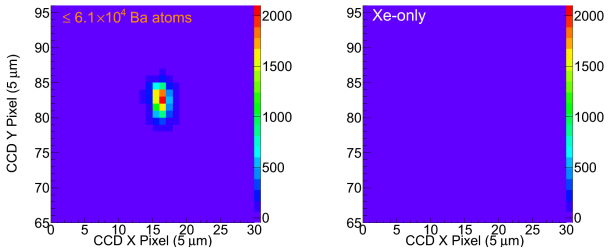

FIG. 4. Image of a Ba^+ deposit yielding $\leq 6.1 \times 10^4$ Ba atoms with its succeeding Xe-only deposit. Exposures are 0.5 s with around 0.6 mW of 572-nm laser excitation.

beam radius of w = 2.4 μm. Aberrations and vibrations in the collection optics and imperfections in the surface of the sXe layer could contribute to blurring of the image. Relative motion of the laser and the window could also lead to exposure of more Ba atoms than calculated above. The latter effect has been checked by observing images of the focused laser relative to a reference point on the sapphire

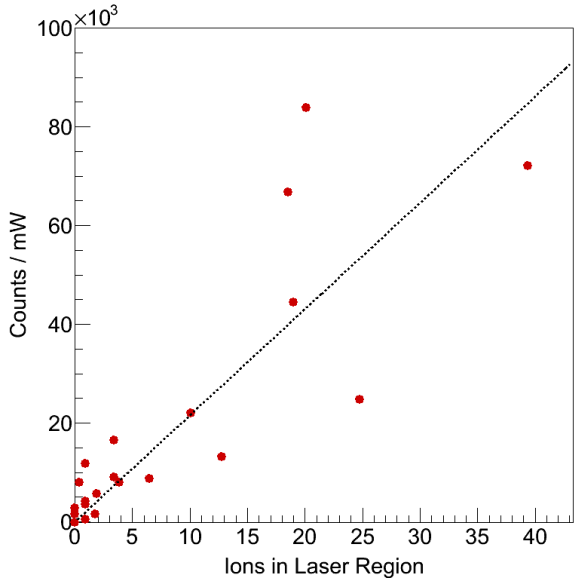

FIG. 5. 619-nm Ba fluorescence vs. number of ions deposited. Exposures are 60 s with around 0.24 mW of 570-nm laser excitation.

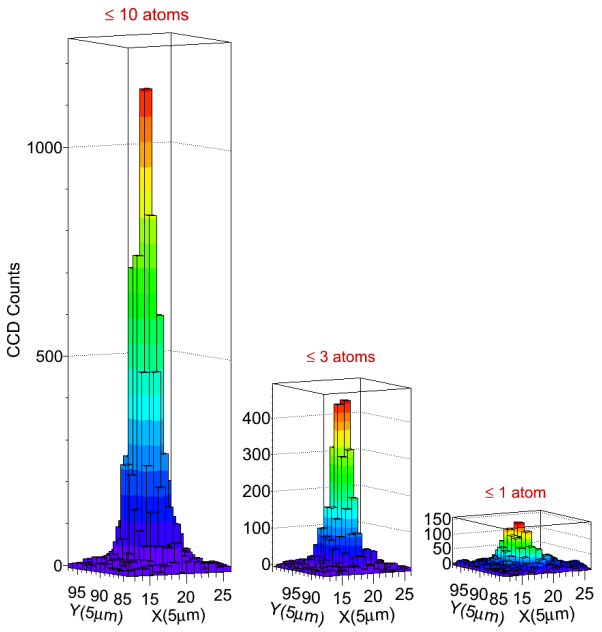

FIG. 6. Subtracted images of 619-nm fluorescence in the focused laser region for runs near the linear trend line in signal vs. ions deposited. Exposures are 60 s with around 0.24 mW of 570-nm laser excitation.

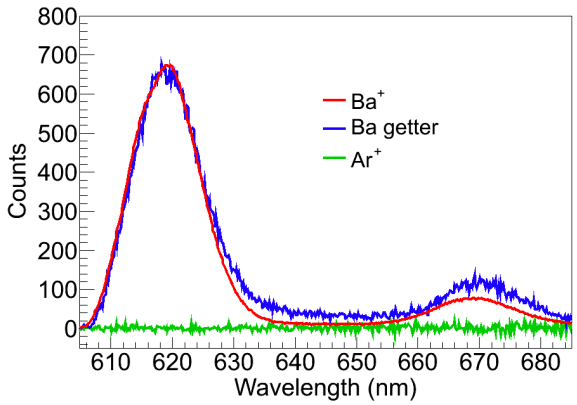

FIG. 7. Observation of deposits from three different sources in sXe. Curves are scaled due to different deposit sizes.

window on time frames down to 50 ms. Sinusoidal vibrations were observed on the order of 12 μm in x and 5 μm in y, due to cryostat vibrations, which corresponds to a total coverage of about 4.7 times the laser region. However, the signal at a given time still comes from an area the size of the laser region. Thus, the signals observed correspond to the above-quoted instantaneous number of Ba atoms illuminated according to the laser spot size, though the total number of atoms illuminated is about 4.7 times larger.

A. Identification of 619-nm Peak as Ba in sXe

Spectra of neutral Ba deposits made with the Ba getter source are compared to spectra of a Ba^+ deposit in Fig. 7. Identical spectra are observed using the different sources under similar deposit conditions. This confirms that the images measured are of Ba atoms resulting from neutralization of the incident Ba^+ ions. Another peak at 670 nm which is mentioned in [7] is also attributed to Ba. No similar fluorescence is observed from deposits of Ar^+ ions in sXe (Fig. 7) at 2000 eV under the same conditions. This rules out matrix damage, e.g. fluorescent color centers, as the source of the 619-nm peak.

B. Backgrounds

Very low concentrations of Cr^{3+} in the sapphire bulk (sub-ppb level) produce a broad fluorescence the tail of which enters the 610-630 nm region passed by the band-pass filter and produces the faintly visible line through the sapphire window discussed above. This fluorescence is identified as Cr^{3+} by its excitation spectrum, identical to that of the well-known lines around 693 nm. Commercially available c-plane quality sapphire from Meller Optics has sufficiently low concentrations for detecting single Ba atoms.

Another background is observed on the surfaces of the window. This emission exhibits bleaching, which can be a challenge for background subtractions. To minimize the surface background, the window is exposed to the laser until the background reaches a steady value, prior to a series of measurements. The set of deposits used for Fig. 5 was done after about an hour of pre-exposure of the sapphire window to the focused laser.

IV. CONCLUSIONS

The 619-nm emission peak observed in deposits of Ba^+ and Ba in sXe is attributed to neutral Ba in a stable and relatively abundant matrix site. Images of 619-nm fluorescence in a focused laser region from Ba atoms are achieved down to an average number of Ba atoms at the single-atom level. Successful detection of Ba atoms in sXe at this level is a significant step toward Ba tagging in nEXO.

ACKNOWLEDGEMENTS

This material is based upon work supported by the National Science Foundation under Grant Number PHY-1132428 and the U.S. Department of Energy, Office of Science, Office of High Energy Physics **under Award Number DE-FG02-03ER41255.**

[1] K.A. Olive *et al.* (Particle Data Group), *Chin. Phys. C* **38**, 090001 (2014) (http://pdg.lbl.gov).
[2] J. Albert *et al.* (EXO-200 Collaboration), *Phys. Rev. C* **89**, 015502 (2014).
[3] J. Albert *et al.* (EXO-200 Collaboration), *Nature* **510**, 229 (2014).
[4] M. Moe, Phys. Rev. C **44**, R931 (1991).

[5] K. Twelker *et al.*, Review of Scientific Instruments **85**, 095114 (2014).
[6] T. Brunner *et al.*, International Journal of Mass Spectrometry **379** (2015) 110-120.
[7] B. Mong *et al.*, Phys. Rev. A **91**, 022505 (1954).
[8] J. Albert *et al.* (EXO-200 Collaboration), *Phys. Rev. C* **92**, 045504 (2015).
[9] Thorlabs part ASL10142-A.